

EXPERIMENTAL PERFORMANCE OF HSC COLUMNS UNDER CYCLIC LOADS

Y. H. HAMMAD¹; M. EISSA²; G. T. ABDEL-RAHMAN³ and M.SAID⁴

¹ Professor of Reinforced Concrete Structures, Faculty of Engineering in Shoubra, Benha Univ., Egypt

² Professor of Reinforced Concrete Structures, Faculty of Engineering, Cairo University, Egypt

³ Associate Professor, Civil Engineering Dept., Faculty of Engineering in Shoubra, Benha Univ., Egypt

⁴ Assistant Lecturer, Civil Engineering Dept., Faculty of Engineering in Shoubra, Benha University, Egypt

ملخص البحث

يهدف هذا البحث لدراسة تصرف السلوك الانشائي للاعمدة ذات الخرسانة عالية المقاومة التي تحتوي على ألياف الصلب والمقيدة بكانات تحت تأثير الاحمال المحورية وأحمال دوريه متغيرة الاتجاه عند منتصف ارتفاع العمود. حيث تم اختبار عدد (14) عينه بأبعاد (1.80*1.80*0.20) وقد تم دراسة بعض المتغيرات التي تؤثر على سلوك هذه العينات ومنها : اختلاف نسبة ألياف الصلب في العينات، قيمة اجهاد الخرسانة، نسبة الاحمال المحورية. وقد اظهرت النتائج ان استخدام الياف الصلب تزيد قيمة الاحمال القصوي واحمال التشرخ وتحسن الممتولية للاعمدة وقد اظهرت النتائج ان افضل نسبة للالياف الصلب هي 1.5%. كما اكدت النتائج انه يفضل ان يكون تأثير الحمل الراسي مأخوذ في الاعتبار وان تكون المعادلة المتاحة في الاكواد معتمدة علي نتائج اعمدة ذات الخرسانة عالية المقاومة عند تصميم الاعمدة الممتولية.

ABSTRACT

The behavior of high strength concrete columns; HSCC with steel fibers under cyclic loading was investigated. Fourteen half-scale column specimens were tested under cyclic lateral load. The key variables covered in this investigation include the steel fibers ratio ranging from 0.00% to 1.50%. The concrete strength varied from 50 MPa to 100 MPa. The columns were subjected to constant axial loads corresponding to target values of 10%, 25% and 45% of the column axial-load capacity. The confinement index values were 0.122, 0.230 and 0.392. The columns were designed according to seismic requirements of ACI 318 Code.

The study present that the steel fibers is shown to improve the performance and ductility of HSC columns. Column with 80% higher amounts of transverse reinforcement than that required by seismic provision of ACI 318-08 and with steel fiber content 1.5% showed ductile behavior and higher ultimate capacity. The results indicated that increasing the axial load level from 10 to 45 percent reduced the maximum displacement by 34 percent. The need to include the axial-load level in ACI Code requirements for confinement reinforcement is pointed out.

KEYWORDS: HSC, HSCC, Fibers, Ductility, Drift, Columns, Cyclic.

1. INTRODUCTION

The use of high-strength concrete has been steadily increasing due to its many advantages over normal-strength concrete. HSC is used primarily in high-rise buildings to significantly decrease the dimensions of the columns in lower stories, thereby reducing the volume of concrete. Studies have shown, however, that HSC is more brittle than NSC [1, 2]. Brittle behavior of high strength concrete in compression has to some extent, limited its application in seismically active regions. Commonly, to overcome the adverse effect of such brittleness on the column behavior, thoughtful confinement is adopted. The

ductility of HSC can also be improved by adding steel fibers to the concrete mass. The maximum volumetric ratio of the fibers is bounded by the workability of the fresh concrete [3].

Due in part to a lack of test results, the New Zealand Standard NZS 3101 [4] and the Canadian Code CSA A23.3 [5] limited the maximum strength that can be used for seismic design to 70 MPa and 55 MPa, respectively. Confinement requirements of ACI Code 318 were originally derived from experimental results from NSC and are not adapted to HSC columns, [6, 7]. Also, it had been shown that HSC columns reinforced according to current code requirements behave in a ductile manner if the axial load is less than 20% of the columns axial load capacity, [6].

Sheikh et al. [7] observed lower ductility in HSC columns as compared to NSC columns concluding that the required amount of tie steel for a given performance of a column under a certain axial load level is proportional to the concrete strength. Paultre et al. [8] demonstrated that the axial load level should be included in ACI requirements for confinement reinforcement. Limited number of tests on HSC columns under cyclic flexure and significant axial compression were reported. Specifically with axial-load in the range of 20% to 40% of column axial-load capacity has been published in literature. Also, most of the available information based on experimental testing of small scale FRHSC columns subjected to concentric axial load only [9].

The objective of this study was to evaluate the steel fibers in enhancing the ductility and load-carrying capacity of HSC columns. The test results not only fill the gap of full-scale test data, but also contribute to the future development of design guidelines for earthquake resistant high strength concrete structures. Also, the study addressed the adequacy of ACI code [10] requirements for seismic design of HSC columns.

2. EXPERIMENTAL PROGRAM

Columns specimens were tested under combined axial load and increasing lateral cyclic load in order to simulate the case of seismic action. The ductility of columns was designed according to seismic requirements of ACI 318 Code. The parameters investigated include the amount of steel fibers, the concrete compressive strength, the axial load level and the confinement index.

2.1 Column Specimens

The experimental program consisted of fourteen half-scale column specimens with a square shape of dimensions 200 x 200 mm and a height of 1800 mm. The specimen represents half of the upper and lower column together with stub representing a small portion of the floor beam. Typical concrete dimensions and reinforcement details of the test specimens are illustrated in Fig. 1. Table 1 shows the details of the test specimens. Three concrete Mixes were designed to achieve a target cubic strength of 50, 75 and 100 N/mm², respectively. Steel fiber with a maximum of 1.5% volumetric ratio was added to the concrete mix. The fiber used in this study was corrugated steel fibers with fiber length of 50 mm and diameter of 0.5 mm. High strength steel-deformed type; grade 40/60 and mild steel-smooth type; grade 24/35 were used in the experimental tests. Detailed characteristics of the materials and mix design are presented in reference [11].

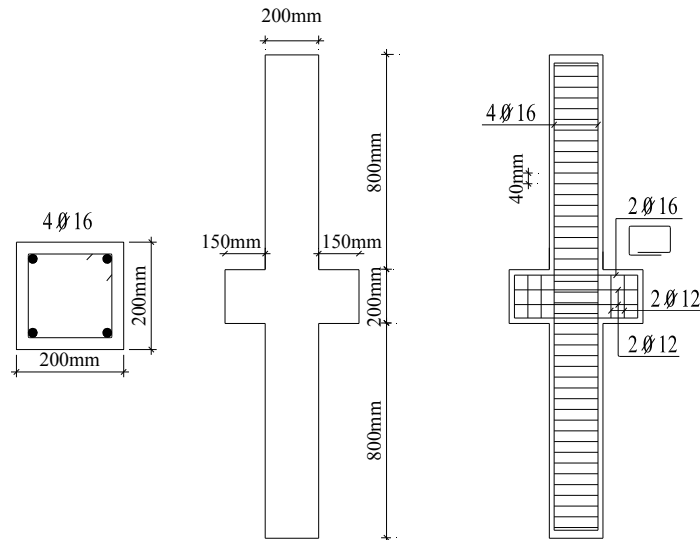


Fig. 1: Typical concrete dimensions and steel reinforcement

Table 1: Details of test specimens

Specimen	Concrete compressive strength (MPa)	Axial load level (P/P_0)	Steel fibers $V_f\%$	Transverse RFT.			
				Bar size (mm)	Yield strength (MPa)	$\rho_s f_{yh}/f_{cu}'$	Volumetric ratio $\rho_s\%$
C1	51.3	0.25	0.00	8	298	0.127	2.13
C2	53.8	0.25	0.75	8	298	0.127	2.13
C3	54.5	0.25	1.50	8	298	0.127	2.13
C4	73	0.25	0.00	10	274	0.122	3.34
C5	76.4	0.25	0.75	10	274	0.122	3.34
C6	77	0.25	1.50	10	274	0.122	3.34
C7	94.7	0.25	0.00	10	516	0.172	3.34
C8	98.6	0.25	0.75	10	516	0.172	3.34
C9	99.8	0.25	1.50	10	516	0.172	3.34
C10	99.6	0.10	1.50	10	516	0.172	3.34
C11	77.6	0.25	1.50	12	613	0.392	4.80
C12	77.1	0.1	1.50	10	274	0.122	3.34
C13	77.3	0.25	1.50	10	516	0.230	3.34
C14	77.9	0.45	1.50	10	274	0.122	3.34

2.2 Test Setup

The test setup consisted of two independent reaction frames for application of lateral and axial loading. The lateral load was applied through a large-scale reaction frame. The axial load was applied through a closed horizontal reaction frame. The specimens were supported on two vertical concrete blocks. The upward reaction is transmitted to the cross girder of the portal frame through hydraulic cylinders mounted to the cross girder; (reversed hydraulic jack and clamping jack). The cylinder at the clamping jack was attached to end ball bearing to permit rotation in case of upward force. Fig. 2 illustrates the details of the setup. The specimens were tested under quasi-static displacement control technique. The standard lateral loading procedure used for all tests is shown in Fig. 3. The required axial load level was applied and kept constant throughout the test. The reversible hydraulic jack, which was controlled by automatic valve, started to apply cyclic lateral load in displacement increments according to the load history stored in the program.



Fig. 2: Test setup

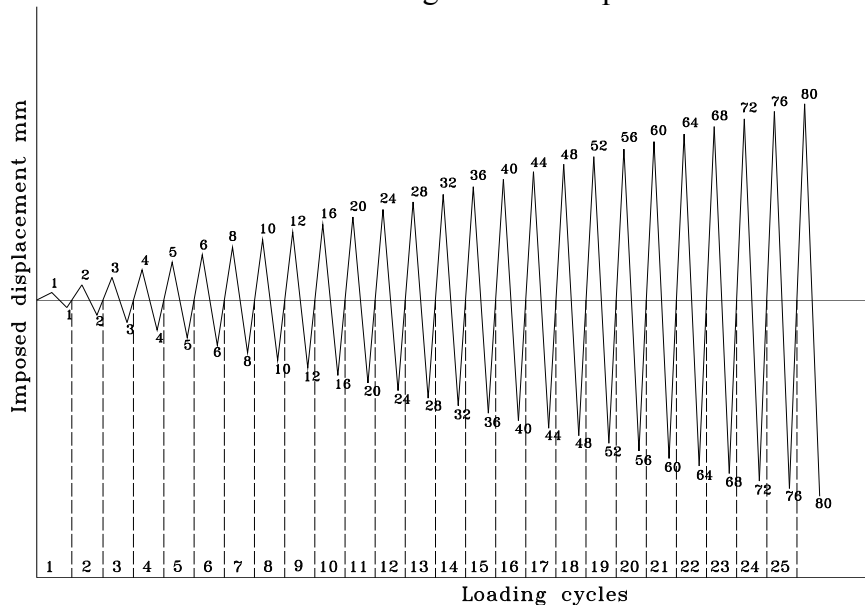


Fig. 3: Cyclic load history

3. TEST RESULTS

3.1 Cracking Behavior

All the specimens experienced the formation of fine flexural cracks in the column at low levels of displacements ranged from 2 to 3 mm near the beam stub. Symmetrical crack patterns occurred for both loading directions. The cracks spread along the columns to a distance of about 400 mm measured from the stub. The cracking load of the specimens without steel fibers ranged from 38 percent to 47 percent of the ultimate load and from 42 percent to 57 percent for columns specimens provided with steel fibers, see Table 2. At the early stages of loading, the width of the cracks developed in the specimen with concrete compressive strength of 75 and 100 N/mm² was smaller than that developed in the specimens with compressive strength of 50 N/mm². Fig. 4 shows the crack propagation of the test Specimen C6.

Table 2: Test results: critical loads, displacements and ductility parameters

Specimen	Cracking level		Ultimate level		Failure level*		Displacement ductility μ_{Δ}	Drift ratio %	Plastic length (mm)
	Δc (mm)	Load (KN)	Δu (mm)	Load (KN)	Δf (mm)	Load (KN)			
C1	2.0	75.0	11.9	200.0	31.0	160.0	6.2	3.9	160.0
C2	2.4	109.0	12.0	251.0	28.0	200.8	4.0	3.5	130.0
C3	2.8	118.0	12.0	257.0	30.0	205.6	4.3	3.8	80.0
C4	2.0	112.0	8.0	240.9	19.7	193.0	3.6	2.5	140.0
C5	2.3	127.0	8.0	282.0	21.5	225.6	4.1	2.7	120.0
C6	2.6	156.0	12.0	289.0	24.0	247.0	4.4	3.0	70.0
C7	2.0	132.0	10.0	288.8	12.0	231.0	2.5	1.5	110.0
C8	2.0	154.0	8.0	332.0	18.0	265.6	4.4	2.2	80.0
C9	2.1	168.0	6.0	343.0	16.5	274.5	4.3	2.1	60.0
C10	2.0	121.0	16.0	289.0	27.5	231.2	4.6	3.4	50.0
C11	2.1	174.0	10.0	359.0	31.6	287.2	7.0	4.0	80.0
C12	2.0	122.0	16.0	239.6	31.5	191.2	7.9	3.9	60.0
C13	2.3	170.0	12.0	344.8	28.0	275.2	7.0	3.5	50.0
C14	3.0	184.0	10.5	328.0	17.0	262.4	3.1	2.1	70.0

* Recorded at 80 percent of ultimate load.

3.2 Mode of Failure

All the specimens failed by crushing of the concrete followed by buckling of the longitudinal bars in the compression zone nearby the column stub. There, the column stirrups were opened. The splitting plane between the concrete cover and the core was

observed to be quite smooth due to cracks passing through the aggregate. Paultre *et al.* [12] pointed out similar mode of failure for tested columns. All the columns were heavily damaged nearby the stub. Fig. 5 depicts the plastic hinge zone for Specimen C2 at the end of the test. Overall, the final failure of HSC specimens without steel fibers was characterized by developing flexural plastic hinge over an average length equal to approximately 55% to 80% of the section depth. Referring to Table 2, the extent of the plastic hinge decreased as the compressive strength increased. A typical observation was recorded for HSC tested Specimens C1, C4 and C7, where demolishing of concrete core inside the stirrups was observed.

The length of plastic hinge of FRHSC Specimens C10 and C12 was 25% and 30% of the section depth. The extent of the plastic hinge decreased as the compressive strength increased, Table 2. The specimens provided with steel fibers, in general, displayed little degree of concrete spalling compared to HSC specimens and damage of the concrete core was not observed during the test. The plastic hinge of Specimen C14 extended over a distance about 35% of the section depth.



Fig. 4: Cracks pattern of test Specimen C6



Fig. 5: Test Specimens; C2 at failure

3.3 Load Displacement Hysteresis Loops

Fig. 6 present the experimental load displacement hysteresis loops for Specimen C12. Generally, the load displacement hysteresis loops for all the test specimens exhibited similar features. For the initial small amplitude cycle, the response was almost elastic and minor residual displacement was observed.

Beyond the ultimate load level, in general, the column strength started to decrease at different rates according mainly to the axial load level. The reduction in the capacity of Specimen C14 that was tested under $P/P_o=0.45$ was more pronounced than that of the corresponding specimens; Specimens C6; ($P/P_o=0.25$), and C12; ($P/P_o=0.10$). To some extent, the FRHSC specimens exhibited improved load displacement response compared to the HSC specimens. A close examination of the strain measurements in the plastic hinge zone reveals that, the longitudinal bars in tension zone yielded before the ultimate load was reached. The maximum strain in the longitudinal bars was 0.016 as recorded for Specimen C4. The maximum recorded strain in the steel stirrups was 0.00615 for the specimen tested at $0.45P_o$.

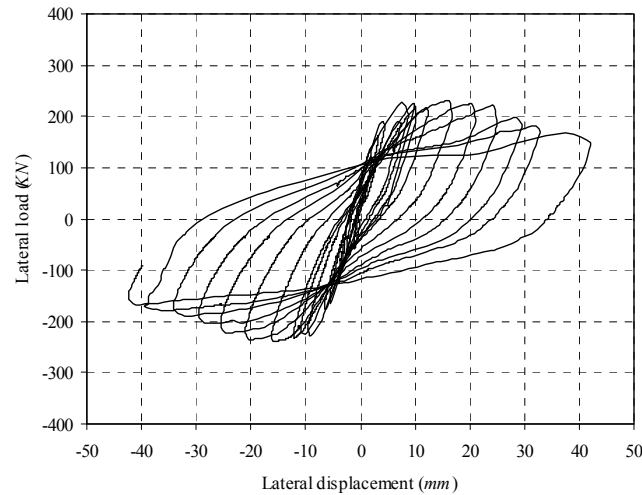


Fig. 6: Load-displacement hysteresis loop of Specimen C12

4. EFFECT OF PARAMETERS

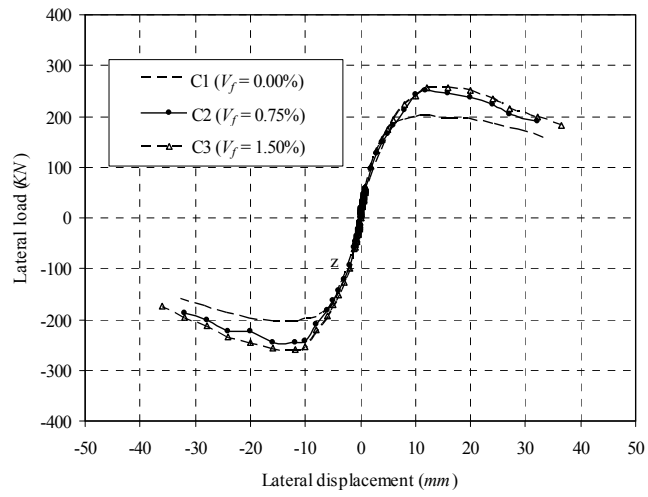
An evaluation is presented for the key column variables that affect the seismic behavior of HSC columns. The following discussion includes the effect of the steel fibers content, concrete compressive strength, axial load level, and confinement index, on the specimen's behavior including the column capacity and the ductility characteristics.

4.1 Steel Fibers Content

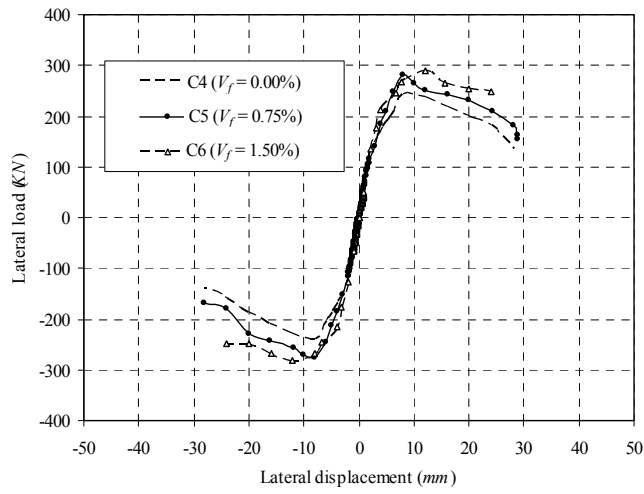
Three groups were tested to study the effect of the amount of steel fibers on the behavior of columns. For specimens with concrete compressive strength of 50 N/mm², the test results show significant improvement in the cracking and ultimate load-carrying capacities of FRHSC columns. Compared to Specimen C1, the increase in the cracking load was 46% and 58%, and in the ultimate load was 26% and 29% for Specimens C2 and C3, respectively, Table 2. Fig. 7a shows the load displacement envelope of Specimens C1, C2 and C3.

As far as specimens with concrete strength of 75 N/mm² are concerned, the increase in the cracking and ultimate load was 13% and 17%, respectively for Specimen C5 ($V_f = 0.75\%$) whereas the corresponding enhancement for Specimen C6 ($V_f = 1.5\%$) was 39% and 20%, respectively, Table 2. Fig. 7b shows the load displacement response of Specimens C4, C5 and C6. The extent of the plastic hinge of Specimens C5 and C6 was 86% and 50% of that of Specimen C4.

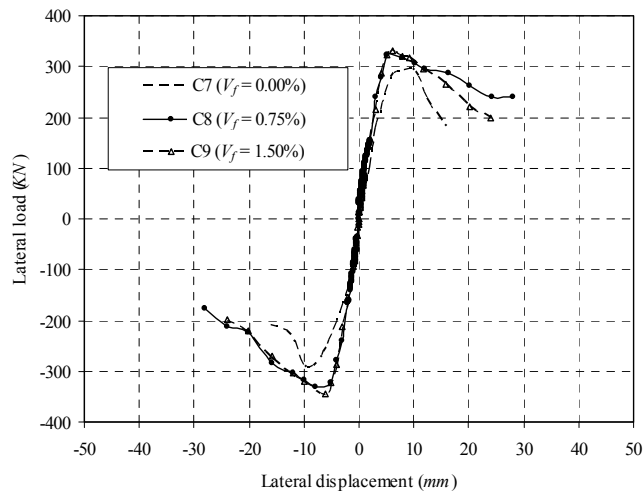
Test results of specimens with concrete compressive strength of 100 MPa reveal that the cracking load increased by 17% and 27%, for specimens with 0.75% and 1.5% steel fibers ratio, whereas the enhancement in the ultimate load was 15% and 19%, respectively. Fig. 7c shows the load displacement envelope of Specimens C7, C8 and C9. As shown, provision of steel fibers increases the displacement ductility by about 76% and the drift ratio by 47%. The improvement in the cracking and ultimate load-carrying capacity is due to the steel fibers are superior in increasing the tensile and bond strength as well as the confinement of the concrete core. Paultre *et al.* [13] concluded that the reduction of the amounts of confinement steel seems to be possible when using FRNSC.



a)



b)



c)

Fig. 7: Effect of fiber content on load-displacement response of specimens with nominal concrete strength: a) 50 MPa; b) 75 MPa; c) 100 MPa

4.2 Concrete Compressive Strength

Test results on ten specimens; C1 to C9 and C13, were analyzed to demonstrate the effect of concrete compressive strength on the column behavior. All the specimens were designed based on the minimum requirements of the seismic provisions of ACI 318 as set on the transverse reinforcement, except Specimen C13 which had 80% additional capacity of the transverse steel.

Fig. 8a shows the load-displacement response of specimens without steel fibers; Specimens C1, C4 and C7. Increasing the concrete compressive strength from 51.3 MPa to 73.0 MPa and 94.7 MPa resulted in 50% and 76% increase in the cracking load, respectively, and in 20% and 44% enhancement in the ultimate load, respectively, Table 2. Obviously, the cracking capacity depends mainly on the concrete strength whereas the ultimate flexural capacity is significantly affected by the reinforcement content. Specimen C1 with 51.3 MPa concrete strength display a more ductile manner compared to Specimens C4 and C7. It can be concluded that in HSC columns subjected to cyclic lateral load as the concrete strength increases, the displacement ductility and drift ratio decreases.

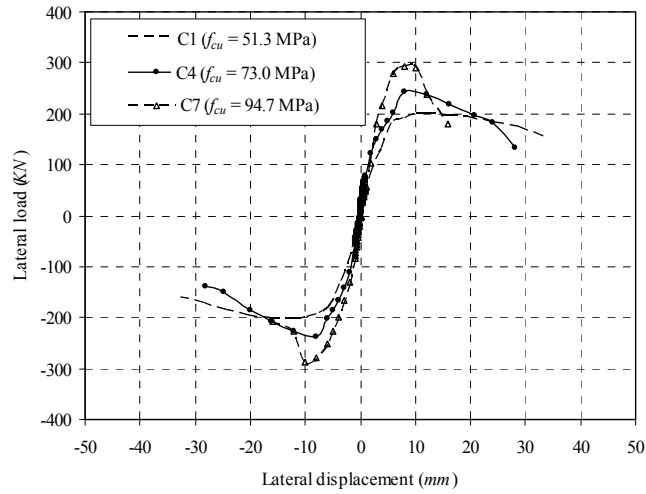
To a lesser extent, a comparable effect of the concrete compressive strength on the column specimens provided with 0.75% fiber content; Specimens C2, C5 and C8, was recorded, Fig. 8b. Compared to Specimen C2, the increase in the cracking load of Specimens C5 and C8 was 17% and 41%, respectively, whereas the increase in the ultimate capacity was 12% and 32%, respectively. The test results reveal a decline in the drift ratio from 3.5 to 2.2 with increasing the concrete strength from 53.8 to 98.6 MPa.

As far as the column specimens provided with 1.5% fibers content; Specimens C3, C6 and C9, are concerned, increasing the concrete strength from 54.5 MPa to 99.8 MPa resulted in an increase in the cracking and ultimate load by 42% and 33%, respectively. Specimen C3 with 54.5 MPa concrete strength display a more ductile manner compared to Specimens C6 and C9, see Fig. 8c. The plastic hinge developed in Specimen C3 extended over a length being 14% and 33% more than that of Specimens C6 and C9, respectively, Table 2. The drift ratio dropped from 3.8 to 2.1 with increasing the concrete strength from 54.5 to 99.8 MPa.

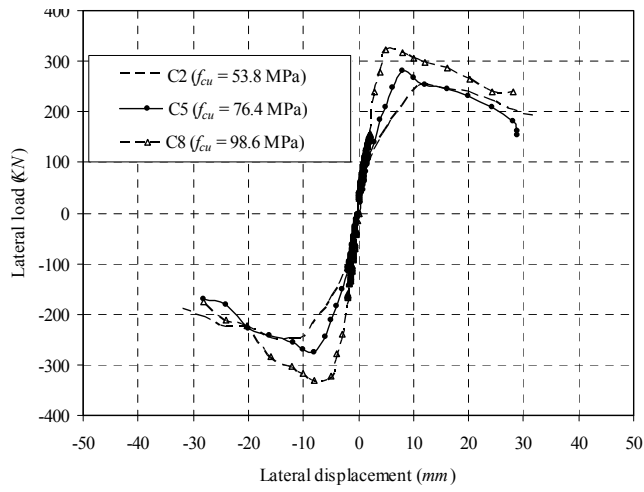
A close examination of the load-displacement response for Specimens C9 and C13 shown in Fig. 8c reveals that the concrete compressive strength has a significant effect on the post-peak response of the test columns. Unlike the previous groups, the change in the column behavior is attributed only to the concrete strength. The results indicate that Specimen C13 with transverse reinforcement of 80% more than the minimum required by ACI 318 developed significantly higher deformability compared to Column C9.

4.3 Axial Load Level

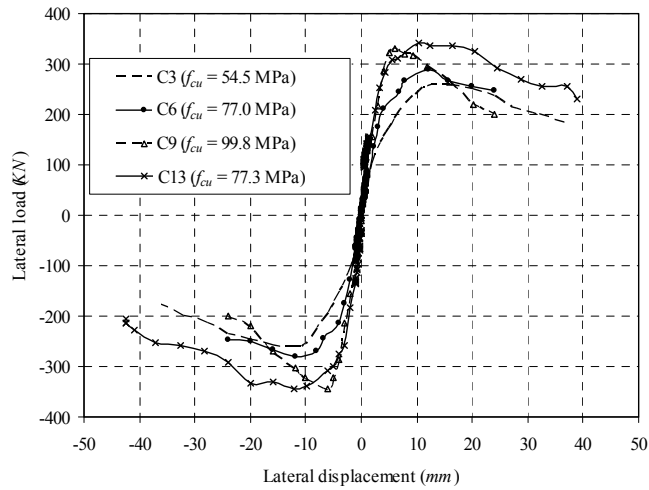
In order to study the influence of the axial load level on the behavior of FRHSC columns, test results on Specimens C6, C9, C10, C12 and C14 were analyzed. These specimens had identical column parameters with concrete compressive strength of 75MPa and 100 MPa, and subjected to axial load of 0.10, 0.25 or 0.45 of the axial load capacity.



a)



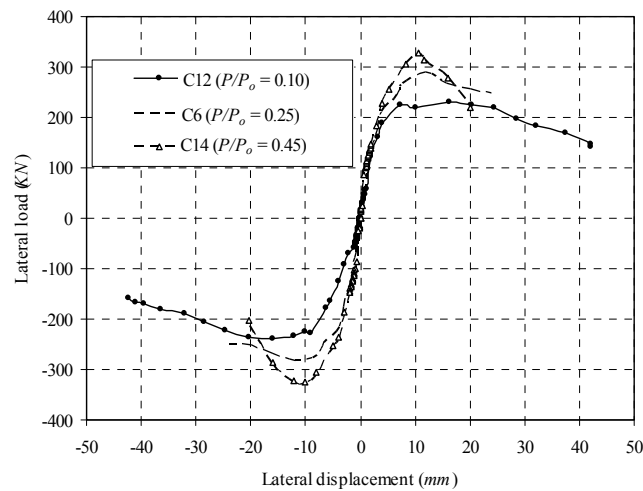
b)



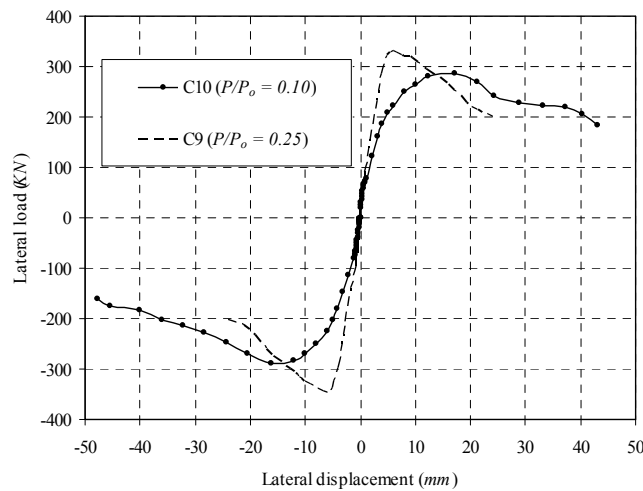
c)

Fig. 8: Effect of concrete compressive strength on load-displacement response of specimens with steel fibers content: a) 0.00%; b) 0.75%; c) 1.50%

For the specimens with nominal concrete strength of 75 MPa, the load carrying capacity is shown in Fig. 9a to increase significantly with increasing the applied axial load from 0.1 to 0.45 of the axial load capacity. The increase in the cracking and ultimate load was 51% and 37%, respectively. In addition, increasing the axial load level from 10 to 45 percent reduced the ultimate displacement from 16 mm to 10.5 mm. Sheikh *et al.* [7] accepted that ACI requirements on confinement reinforcement are not conservative in case of highly axially loaded columns, and rather conservative and uneconomical in a great number of situations of practical interest in which columns support low axial compression.



a)



b)

Fig. 9: Effect of axial load level on load-displacement response of specimens with nominal concrete strength: a) 75 MPa; b) 100 MPa.

Comparable conduct was observed for specimens with nominal concrete strength of 100 MPa; Specimens C9 and C10 as shown in Fig. 9b. The load carrying capacity is shown to increase with increasing the applied axial load from 0.10 to 0.25 of the axial load capacity. The test results reveal that the displacement ductility was 4.6 and 4.3 at an axial load level of 10% and 25%, respectively and the corresponding drift ratio was 3.4 and 2.1, respectively. A close examination of these results reveals that when the level of axial load is 25 percent of the column axial load capacity and the concrete strength is approximately 100 MPa, larger amounts of transverse reinforcement, than specified in the seismic provisions of ACI 318, are required. This agrees with the recommendation of ACI 441 [14] on columns with concrete strength approximately 100 MPa and with axial load level above 30%.

4.4 Confinement Index

This section presents a discussion on the significance of the confinement index $\rho_s f_{yh} / f'_{cu}$ on the behavior of HSC columns. The factor $\rho_s f_{yh} / f'_{cu}$ has been recommended by ACI 441 to evaluate the confinement efficiency. Test results on Specimens C6, C11 and C13 were investigated to evaluate the effectiveness of the confinement index. The confinement index values were 0.122, 0.392 and 0.230. Fig. 10 shows the load-displacement response of these specimens. The increase in the cracking load was about 11% and the corresponding enhancement in the ultimate load was 24%, Table 2. With increasing the confinement index from 0.122 to 0.392 the drift ratio increases from 3.0 to 4.0. The ratio $\rho_s f_{yh} / f'_{cu}$ can be used as a design parameter for the confinement of HSC columns.

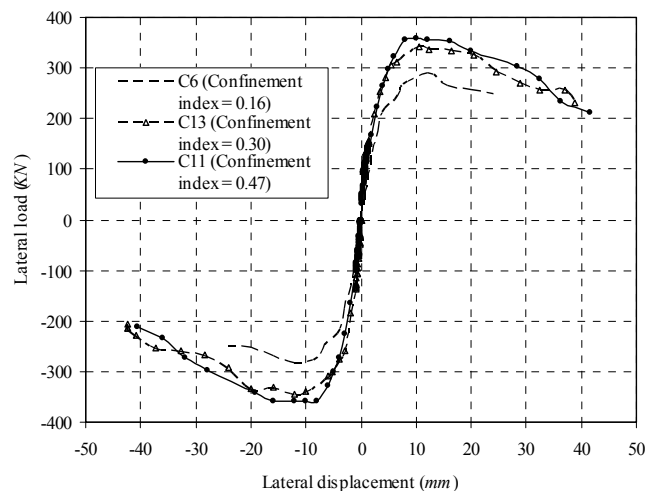


Fig. 10: Effect of confinement index on load-displacement response

5. CONCLUSIONS

The main findings from the test results of the half-scale HSC and FRHSC columns subjected to axial load and cyclic lateral forces can be summarized as follows:

1. Provision of the steel fibers enhanced the cracking load, ultimate capacity and the ductility of the test columns. The maximum enhancement of the performance of FRHSC columns is achieved with a steel fiber content of 1.5% in volume fraction. The recorded enhancement in the ultimate capacity due to introducing the steel fibers, ranged from

15% to 29% according to the steel fiber content and the concrete strength. Near the failure stage, the specimens with steel fibers had wider cracks compared to the cracks in the specimens without steel fibers.

2. Increasing the axial load level from 10 to 45 percent reduced the maximum displacement by 34 percent and increased the cracking and ultimate load by 51% and 37%, respectively, for columns with concrete compressive strength of 75MPa, whereas, for concrete compressive strength of 100MPa, increased the axial load level from 10 to 25 percent reduced the maximum displacement by 62 percent and increased the cracking and ultimate load by 39% and 19%, respectively.

3. An increase in axial load reduces the column deformability and ductility and accelerates strength and stiffness degradation with every load cycle. Therefore, the axial load level should be incorporated as a design parameter in the design of confinement reinforcement.

4. Columns that had approximately 50 MPa concrete and axial loads level of 25 percent of column axial load capacity, and that were designed based on seismic provisions of ACI 318, exhibited adequate ductility. Columns with concrete compressive strength about 75 MPa and with axial load beginning from 25 percent of column axial load capacity require higher amounts of transverse reinforcement than required by seismic provisions of ACI 318 to attain the ductility level intended by the code.

5. The confinement index ratio is one of the key parameters affecting deformability of HSC columns.

6. Though the columns were all compared with the current ACI 318 code requirements for transverse reinforcement in the potential plastic hinge regions of a column, the test results show that the current code provision appeared to be over conservative for lower axial load levels and normal strength concrete, but less conservative for higher axial load levels and high strength concrete.

REFERENCES

1. Cusson, D., and Paultre, P., (1994), "High-Strength Concrete Columns Confined by Rectangular Ties," *Journal of Structural Engineering*, ASCE, V. 120, No. 3, pp. 783-804.
2. Razvi, S. R., and Saatcioglu, M., (1994), "Strength and Deformability of Confined High-Strength Concrete Columns," *ACI Structural Journal*, V. 91, No. 6, Nov.-Dec., pp. 678-687.
3. Foster, S. J. and Attard, M., (2001), "Strength and ductility of fiber reinforced high-strength concrete columns," *ASCE Journal of Structural Engineering*, V. 127, No. 1, Jan., pp. 28-34.
4. NZS 3101-95 - Part I, (1995), "Code of Practice for the Design of Concrete Structures," Standards Association of New Zealand, Wellington, New Zealand.
5. CSA A23.3, (2004), "Design of Concrete Structures for Buildings (CSA A23.3-04)," Canadian Standards Association. Mississauga, ON, Canada.
6. Azizinamini, A., Baum Kuska, S. S., Brungardt, P. and Hatfield, E., (1994), "Seismic behavior of square high-strength concrete columns," *ACI Structural Journal*, V. 91, No. 3, May-June, pp. 336-345.
7. Sheikh, S. A., Shah, D. V., and Houry, S. S., (1994), "Confinement of high-strength concrete columns," *ACI Structural Journal*, V. 91, No. 1, Jan.- Feb., pp. 100-111.
8. Paultre, P., Eid, R., Robles, H., I. and Bouaanani, N., (2009), "Seismic performance of circular high strength concrete columns," *ACI Structural Journal*, V. 106, No. 4, July-Aug., pp. 395-404.

9. Sharma, U., K., Bhargava, P., and Sheikh, S. A., (2007), "Tie-confined fibre-reinforced high-strength concrete short columns," Magazine of Concrete Research, V.59, No. 10, Dec., pp.757-769.
10. ACI Committee 318, (2008), "Building code requirements for reinforced concrete (ACI 318-08) and commentary (ACI 318R-08)," American Concrete Institute, Farmington Hills, Mich.
11. Said, M., (due 2010), "Structural Behavior of High Strength Concrete Columns under Cyclic Loads," Ph.D. Thesis, Faculty of Engineering in Shoubra, Benha University, Cairo, Egypt.
12. Paultre, P., Legeron, F., and Mongeau, D., (2001), "Influence of concrete strength and transverse reinforcement yield strength on behavior of high-strength concrete columns," ACI Structural Journal, V. 98, No. 4, July-Aug., pp. 490-500.
13. Paultre, P., Proulx, J., Elwood, K., and Roy, N., (2008), "Behavior of synthetic fiber-reinforced concrete circular columns under cyclic flexure and constant axial load," Report, Department of Civil Engineering, University of Sherbrooke, Canada.
14. ACI-ASCE Committee 441, (1997), "High-Strength Concrete Columns: State-of-the-art," ACI Structural Journal, V. 94, No. 3, May-June, pp. 323-335.